C–H Bond Activation In Ribonucleotide Reductases—Do Short, Strong Hydrogen Bonds Play a Role?

M. Mohr and H. Zipse*[a]

Abstract: The hydrogen-transfer reactions between methyl thiyl radical and methanol, ethylene glycol, and 3,4-dihydroxytetrahydrofuran have been studied as model systems for the C–H bond activation step in ribonucleotide reductases with DFT methods. In all three cases, the overall reaction is endothermic. The lowest reaction barrier and the smallest endothermicity has been found for the tetrahydrofuran substrate. The influence of hydroxide, formate, hydronium, and neutral formic acid on the C–H bond activation in ethylene glycol has also been studied. Taking the reduction of the intrinsic barrier height as a measure of catalytic activity, the negatively charged formate group is the most effective catalyst. This catalytic effect is based on the formation of a strong anionic hydrogen bond, which achieves its maximum strength in the transition state of the C–H bond activation step. The observed modulation of the hydrogen bond strength along the reaction pathway is ultimately traced back to the electrophilic nature of the methyl thiyl radical.

Keywords: C–H bond activation · density functional calculations · radicals · ribonucleotide reductase · sulfur

Introduction

The mechanism of the ribonucleotide reductase (RNR) catalyzed reduction of ribonucleotides to the corresponding desoxy ribonucleotides has been debated for years.[1–5] While much of the discussion has centered on the dramatically different cofactors found in different classes of RNRs,[1, 3–5] the unusual interplay of homo- and heterolytic bond cleavage steps proposed in the actual nucleotide reduction process in class I and II RNRs has contributed its share of controversy. One currently accepted working hypothesis includes the five steps depicted in Scheme 1.

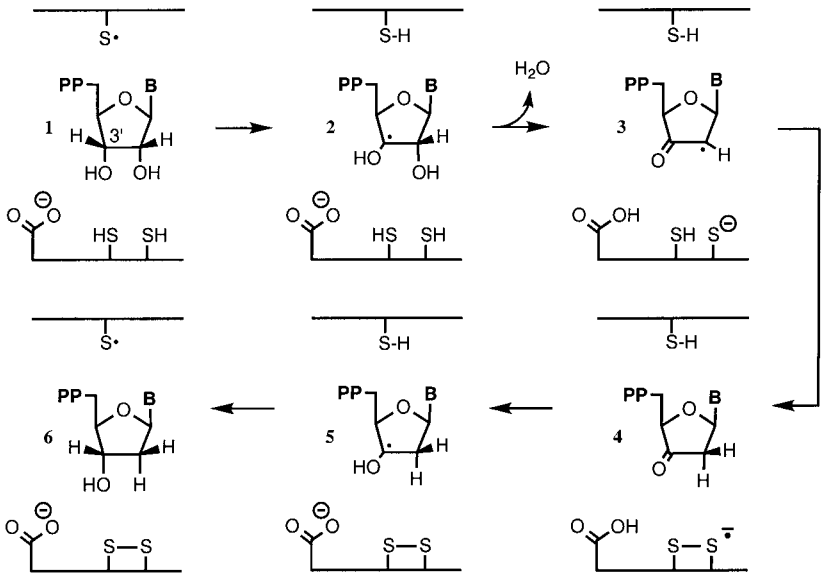

Scheme 1.

After the binding of the diphosphate substrate **1** into the active site of the enzyme, the first chemically significant step involves hydrogen abstraction from the nucleotide 3′ carbon atom through a thiyl radical derived from cysteine residue CYS439. The 3′-radical **2** formed in this process then undergoes elimination of water to yield the α-keto radical **3**. Reduction of this radical through thiol groups situated in the active site yields the closed shell derivative **4**, which is

[a] Prof. H. Zipse, M. Mohr
Institut für Organische Chemie, LMU München
Butenandt-Str. 13, Haus F, D-81377 München (Germany)
Fax.: (+49) 89-2180-7738
E-mail: zipse@cup.uni-muenchen.de

Supporting information for this article is available on the WWW under http://www.wiley-vch.de/home/chemistry/ or from the author.

0947-6539/99/0510-3046 $ 17.50+.50/0

subsequently reduced to the modified 3′-radical **5**. The final step involves the reinstatement of the hydrogen atom originally removed from the 3′-position to form the reduced ribonucleotide **6**. Several limiting cases have been discussed for the water elimination mechanism from radical **2**. If water elimination occurs in an acid-catalyzed fashion, the protonated radical **7** as well as radical cation **8** might be formulated

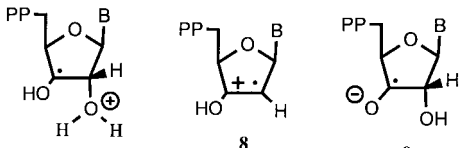

7 **8** **9**

as reaction intermediates.[1b, 3, 4] Similar intermediates have been proposed to occur in the acid-catalyzed water elimination from ethylene glycol.[6] If, however, base catalysis through the GLU441 carboxylate group situated in the active site is operative, the ketyl radical anion **9** should be formed at some point along the reaction pathway.[2] Ketyl radicals such as **9** have been implied in the base-catalyzed water elimination from small α,β-dihydroxyalkyl radicals.[6c, 7] The lifetime of the radical ion intermediates **7**–**9** might, however, be extremely limited, and a fully concerted mechanism devoid of discrete radical ion intermediates might be envisioned as a third mechanistic alternative.[1d, 8] A recent theoretical study by Siegbahn advocates a variation of the concerted step, in which GLU441 in the neutral state (and not in the anionic form depicted in Scheme 1) acts as a bifunctional catalyst for the water elimination step.[9] All of the above scenarios assume the initial C–H bond activation step to be homolytic in nature, despite the fact that this step might not be thermochemically favorable. How unfavorable this reaction step actually is depends on the bond dissociation energies of the 3′-C–H and the cysteine S–H bonds. Assuming C–H bond energies of 92 kcal mol^{-1} (as in secondary alcohols) and S–H bond energies between 82 and 92 kcal mol^{-1}, the hydrogen-transfer step might be endothermic by anywhere between 0 and 10 kcal mol^{-1}.[1d, 10] An exact prediction of the thermochemistry must, however, also consider the state of protonation of the substrate. It has previously been shown in a theoretical study by Steigerwald et al. that the C–H bond energy in methanol is reduced by 16.5 kcal mol^{-1} upon formation of free alkoxide ions and by 10.1 kcal mol^{-1} upon formation of sodium methoxide.[11] Deprotonation of the 3′-hydroxy group in substrate **1** could therefore lead to an exothermic C–H bond activation step. It is, however, not obvious which basic residue located in the RNR active site would be sufficiently potent to effect deprotonation of the 3′-hydroxy group of substrate **1**. That the hydrogen-bonding network present in the RNR active site might also have a significant influence on the C–H bond activation step has been one of the important results of Siegbahn's recent theoretical study.[9] Alternatively, the catalytic activity of RNR might be derived from the combination of an endothermic hydrogen-transfer step with a rapid, irreversible followup reaction.[1d, 2]

In order to clarify the discussion surrounding the initial C–H bond activation step in the RNR-catalyzed reduction of ribonucleotides we have now performed theoretical studies of the reaction between the methyl thiyl radical (**10**) and methanol (**11**), ethylene glycol (**17**), and *cis*-3,4-dihydroxy tetrahydrofuran (**22**). The influence of the state of protonation on the C–H bond activation process has furthermore been explored by the use of ethylene glycol as a model substrate, hydroxide and formate anions as model bases, and the hydronium cation as well as formic acid as model acids. Siegbahn has argued[9] that the use of charged model systems leads to a distorted view in many catalytic systems and has therefore modeled the RNR active site with neutral residues. While it is certainly true that great care must be taken in choosing model systems in general, important aspects of the RNR mechanism of action might be missed by imposing this constraint.

Computational Methods

Calculations were performed at three different levels of theory. At all three levels of theory, the split-valence double-zeta basis set (DZP) optimized by Andzelm and Godbout was used.[12] First, the complete reaction mechanism was investigated at the Hartree–Fock level of theory for closed-shell compounds and at the unrestricted Hartree–Fock level of theory for all open-shell species. This level of theory will be referred to as "UHF/DZP". Using the UHF/DZP optimized structures, we reevaluated the energies at the Becke3LYP level of theory[13] using the 6-311 + G(2d,p) basis set. This basis set will be referred to as "LB" (large basis). The scaled zero-point vibrational energies (factor 0.9) calculated at the UHF/DZP level of theory were included in the calculation of energy differences. This level of theory will be termed "B3LYP/LB//UHF/DZP". The most favorable reaction pathways were then reoptimized at the Becke3LYP/DZP level of theory. Relative energies calculated at this level have been termed "B3LYP/DZP". Energy differences have again been recalculated at the Becke3LYP/6-311 + G(2d,p) level of theory. Combination of these single-point energies with the unscaled differences in Becke3LYP/DZP zero-point energies yield the "B3LYP/LB//B3LYP/DZP" estimates. In order to verify the performance of these inexpensive approaches, the smallest model system studied here has also be studied at two other theoretical levels. First all structures were reoptimized at the Becke3LYP/LB level of theory. Inclusion of the unscaled zero-point energy differences computed at this level of theory gave "B3LYP/LB//B3LYP/LB" relative energies. Relative energies were also computed at the CCSD(T)/cc-pVTZ level with the use of the Becke3LYP/LB geometries. Combination with Becke3LYP/LB zero-point energy differences yielded "CCSD(T)" relative energies. Charge- and spin-density distributions were calculated from a Mulliken population analysis with the B3LYP/DZP orbitals. Spin contamination is a frequent worry in calculations that use unrestricted wavefunctions. In the Becke3LYP calculations performed here, however, the expectation value for S^2 never exceeded a value of 0.76. All calculations were performed with Gaussian 94[14] and MOLPRO 96.[15]

Results

C–H bond activation in neutral systems

Methanol as the substrate: The smallest model system used here to study the initial C–H bond activation step through thiyl radicals consists of the methylthiyl radical (**10**) and methanol (**11**) (Scheme 2, drawn to scale at the B3LYP/LB//B3LYP/DZP level of theory). After hydrogen transfer, the methanol radical (**12**) and methyl thiol (**13**) are formed as the products. The heats of formation of all four species **10**–**13** are known from experiment as well as from previous theoretical

  0947-6539/99/0510-3047 $ 17.50+.50/0

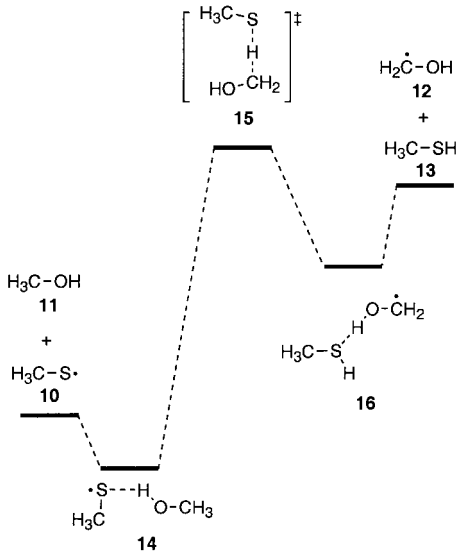

Scheme 2.

studies with G2 theory.[16] Using these previously determined values, we can validate the theoretical methods used in this study. Based on experimental heats of formation, the reaction enthalpy amounts to $\Delta H_{rxn}(298\ K) = +8.8 \pm 1.5$ kcal mol^{-1} at 298 K. From G2 theory, reaction enthalpies of ΔH_{rxn}(G2, 298 K) $= +10.3$ kcal mol^{-1} and ΔH_{rxn}(G2, 0 K) $= +10.1$ kcal mol^{-1} have been calculated at 298 and 0 K, respectively. We may thus conclude that G2 predicts, within experimental uncertainty, the correct reaction thermochemistry and that the thermal correction (0 to 298 K) for this reaction is rather insignificant. We can then use the zero-point energy corrected total energies obtained at various levels of theory directly to predict the reaction thermochemistry. The use of CCSD(T) energies leads to practically the same reaction energy of $\Delta E_{rxn}(0\ K) = +10.2$ kcal mol^{-1} as obtained at the G2 level. The values of ΔE_{rxn}(0 K) calculated at the B3LYP/LB//UHF/DZP, B3LYP/LB//B3LYP/DZP, and B3LYP/LB//B3LYP/LB levels of theory are +9.5, +9.6, and +9.5 kcal mol^{-1}, respectively (Table 1). Since practically the same value is obtained at all three levels of theory, it appears that variation of the underlying geometries does not lead to significant changes. Also, all three predictions are actually closer to the experimental value by 0.7 kcal mol^{-1} than the G2 and CCSD(T) predictions. These results suggest that reaction energies for the C–H bond activation through thiol radicals will be predicted quite accurately by the use of hybrid density functional methods with medium-sized basis sets.

The reaction between **10** and **11** is initiated through formation of a weak complex **14**, which includes a hydrogen bond between the thiyl radical and methanol. The reaction then proceeds through transition state **15**, located 11.1 kcal mol^{-1} (B3LYP/LB//B3LYP/DZP) above the reactants, to product complex **16**. The latter is again characterized through a hydrogen bond between the hydroxy group of the methanol radical and the sulfur atom of methyl thiol. Owing to stronger hydrogen bonding in **16** than in **14** the energy difference between the reactant and product complex of $\Delta E = +8.4$ kcal mol^{-1} is slightly smaller than the reaction energy. The level of theory chosen for geometry optimization does have a larger influence on the calculated reaction barrier than on the reaction energy noted before (Table 1). While an identical barrier of +11.1 kcal mol^{-1} is predicted at the B3LYP/LB//B3LYP/DZP and B3LYP/LB//B3LYP/LB levels of theory, the B3LYP/LB//UHF/DZP barrier is 0.7 kcal mol^{-1} lower at +10.5 kcal mol^{-1}. Despite the fact that this deviation is still rather small, in the following we will discuss only the results obtained at the B3LYP/LB//B3LYP/DZP level of theory, unless otherwise mentioned.

The structure of transition state **15** is well within expectation (Figure 1). Hydrogen transfer occurs in an almost perfectly collinear fashion at an S–H–C angle of 173.2°, the hydrogen atom being located 1.478 Å from the sulfur and 1.597 Å from the carbon atom. Considering the rather different values for the C–H bond length in methanol (1.099 Å) and the S–H bond length in methyl thiol (1.350 Å), this implies that C–H bond breaking as well as S–H bond making is far advanced, which classifies **15** as a "late" transition state with respect to carbon to sulfur hydrogen transfer. This is in accord with the endothermic nature of the overall reaction. The thiol C–S bond and the methanol C–O bond are oriented to each other in a *gauche* fashion with a C-S-C-O dihedral angle of 54°, in such a way that the C–S bond points away from the methanol O–H bond. A transition state with the alternative *trans* orientation is energetically less favorable at the UHF/DZP level and could not be located as a stationary point at either the B3LYP/DZP or B3LYP/LB level of theory. The spin-density distribution supports the classification of structure **15** as a late transition state. Most of the spin density is located on the

Table 1. Relative energies [kcal mol^{-1}] for stationary points in the reaction of the methylthiyl radical (**10**) with methanol (**11**), ethylene glycol (**17**), and 3,4-dihydroxytetrahydrofuran (**22**).

Structure	ΔE [UHF/DZP]	ΔE [B3LYP/LB //UHF/DZP]	ΔE [B3LYP/DZP]	ΔE [B3LYP/LB //B3LYP/DZP]	ΔE [B3LYP/LB// //B3LYP/LB]
10[a] + **11**	0.0	0.0	0.0	0.0	0.0
14	−2.6	−2.0	−3.8	−2.3	−2.3
15	+32.4	+10.4	+15.8	+11.1	+11.1
16	+14.2	+6.3	+10.1	+6.1	+6.0
12 + **13**	+17.4	+9.5	+14.9	+9.6	+9.5
10[a] + **17**	0.0	0.0	0.0	0.0	–
19	−2.7	−2.3	−3.9	−2.5	–
20	+32.5	+9.8	+15.3	+10.2	–
21	+13.7	+5.2	+8.7	+4.4	–
13 + **18**	+16.5	+7.3	+11.8	+7.1	–
10[a] + **22**	0.0	0.0	0.0	0.0	–
24	−2.7	−3.0	−4.7	−3.4	–
25	+31.6	+7.6	+12.8	+7.9	–
26	+12.8	+4.3	+7.9	+3.4	–
13 + **23**	+15.8	+6.2	+10.9	+6.1	–

[a] C_s symmetry, A′ state.

0947-6539/99/0510-3048 $ 17.50+.50/0 *Chem. Eur. J.* **1999**, *5*, No. 10

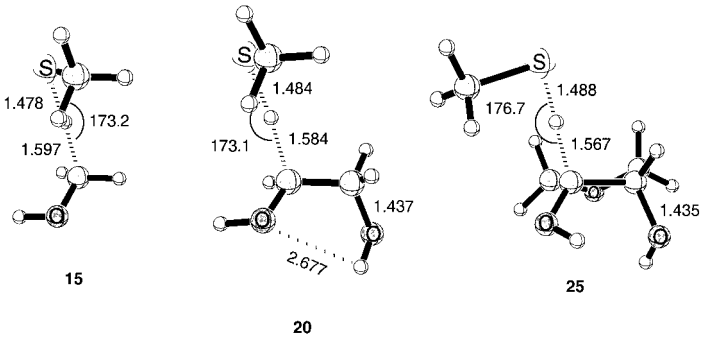

Figure 1. Transition states (**15**, **20**, and **25**) for the hydrogen-transfer reaction between methyl thiyl radical (**10**) and methanol (**11**), ethylene glycol (**17**), and 3,4-dihydroxytetrahydrofuran (**22**), respectively, optimized at the B3LYP/DZP level. Distances are given in Å and angles in degrees.

methanol carbon and oxygen atoms with coefficients of 0.66 and 0.13, respectively. The remaining spin density is located on the sulfur atom with a coefficient of 0.30. Cumulative charges for the CH_3S and CH_3SH moieties in **15** are -0.13 and -0.07 e, respectively. This small charge separation hints towards the mainly homolytic nature of transition state **15**, but also points to the electrophilic character of the methylthiyl radical (**10**).

Ethylene glycol as the substrate: Reaction of ethylene glycol (**17**) with thiyl radical **10** yields the secondary radical **18** and methyl thiol (**13**) as the products (Scheme 3). The higher

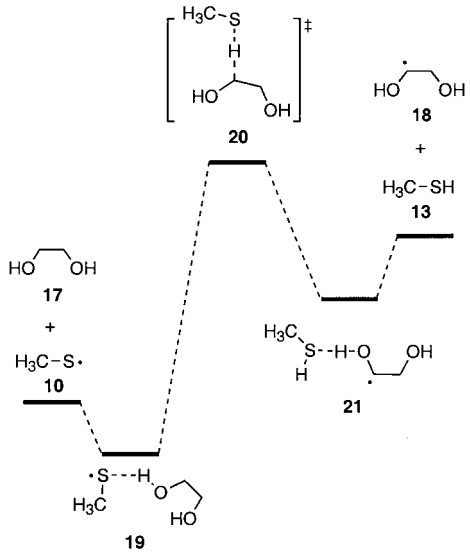

Scheme 3.

stability of radical **18** (relative to **12**) leads to a reaction energy of $\Delta E_{rxn}(0\,K) = +7.1$ kcal mol^{-1}, which is 2.5 kcal mol^{-1} less endothermic than the C–H bond activation in methanol. The reaction follows a very similar pathway as found before for methanol. Formation of a hydrogen-bonded complex **19** is followed by the transition state for hydrogen transfer **20** and the product complex **21**. Hydrogen bonding is comparable in the reactant and product complexes and the energy difference between **19** and **21** of 6.9 kcal mol^{-1} is rather similar to the overall reaction energy. The activation barrier of $+10.2$ kcal mol^{-1} is only slightly lower than the barrier for methanol activation and the basic structural characteristics of the hydrogen-transfer transition state are unchanged (Figure 1). The timing of C–H bond breaking and S–H bond making, and the hydrogen-transfer angle are basically identical in **20** and in **15**. The most favorable orientation of the S–C and C–O bonds is again *gauche* with a dihedral angle of 48.5°. The spin density in **20** is distributed over the S and C atoms involved in the hydrogen-exchange process as well as the α-oxygen atom with coefficients of 0.31, 0.62, and 0.11, respectively. The charges of the CH_3S and CH_3SH moieties in **20** are -0.12 and -0.07 e, respectively. Taken together all these details indicate that hydrogen abstraction from ethylene glycol will be more favorable kinetically and thermodynamically, relative to methanol, with little influence on the transition state structure.

syn-3,4-Dihydroxytetrahydrofuran as the substrate: Reaction of *syn*-3,4-dihydroxy-tetrahydrofuran (**22**) with thiyl radical **10** yields the tertiary radical **23** and methyl thiol (**13**) as the products (Scheme 4). The stability of radical **23** is reflected in

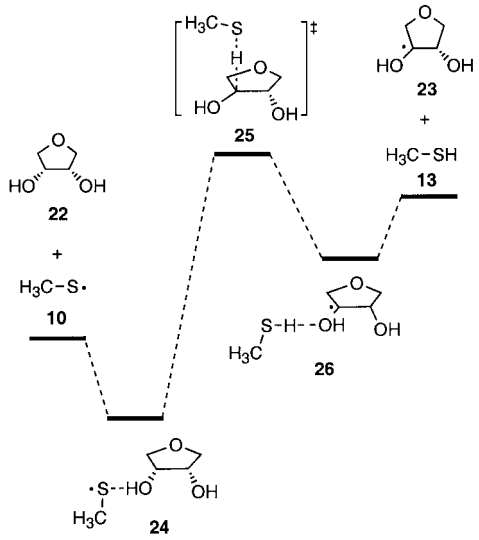

Scheme 4.

the reduced reaction endothermicity of $\Delta E_{rxn}(0\,K) = +6.1$ kcal mol^{-1}. Interestingly, the reaction barrier relative to the separate reactants of $+7.9$ kcal mol^{-1} is significantly lower now than for the two smaller model systems. The reaction barrier starting from complex **24** amounts to 11.3 kcal mol^{-1}. The structure of transition state **25** is, however, still very similar to that of **20** and **15** (Figure 1). As in the case for ethylene glycol, the spin density is distributed over the S and C atoms involved in the hydrogen-exchange process as well as the α-oxygen atom with coefficients of 0.31, 0.61, and 0.12, respectively, and the cumulative charges of the CH_3S and CH_3SH moieties in **25** are -0.11 and -0.09 e, respectively.

In conclusion, these results suggest that hydrogen transfer occurs in a comparable way in all three model systems studied here. The transition states can all be described as "late"

transition states in terms of structural characteristics as well as the spin-density distribution. The smallest endothermicity as well as the lowest reaction barrier has been calculated for the largest substrate **22**. Our best estimate for the endothermicity of the C–H bond activation process in **22** is +6.1 kcal mol^{-1}. The reaction barriers calculated for the three model systems here exceed the reaction thermochemistry by 2–3 kcal mol^{-1}. In the absence of differential binding of the ground and transition state we would thus predict a reaction barrier of approximately 8 kcal mol^{-1} for the RNR-catalyzed reaction, provided that the reaction occurs in a purely homolytic fashion.

Catalysis of C–H bond activation in ethylene glycol

Hydroxide as a catalyst: In order to explore the influence a strongly basic residue might have on the C–H bond activation step, the reaction of radical **10** with ethylene glycol was reinvestigated in the presence of OH^- (Scheme 5).

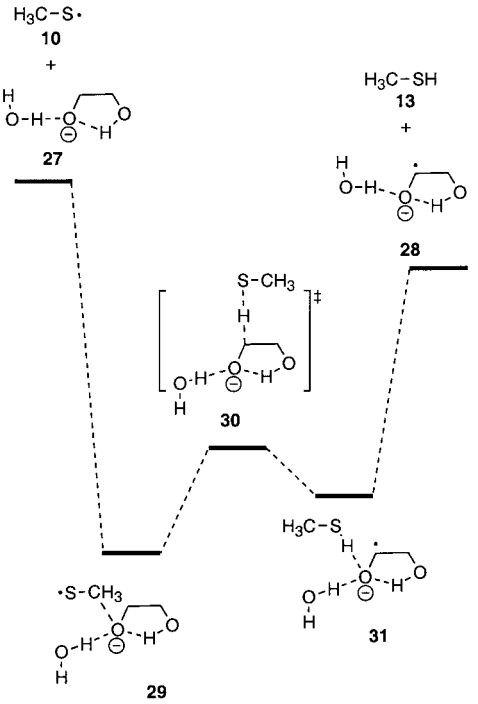

Scheme 5.

The hyrdoxide group reacts with ethylene glycol in the gas phase to give complex **27**, in which a proton has been transferred from ethylene glycol to the hydroxyl anion. Hydrogen abstraction from the carbon atom adjacent to the negatively charged oxygen atom in complex **29** through radical **10** yields radical anion **28** and methyl thiol (**13**). The overall reaction is exothermic by 3.7 kcal mol^{-1}, in marked contrast to the endothermic (by 7.1 kcal mol^{-1}) C–H bond activation reaction of neutral ethylene glycol. This change in reaction energy on going from the neutral to the anionic system is predicted by all theoretical methods used here (Table 2). The change in reaction thermochemistry by 10.8 kcal mol^{-1} is very similar to the theoretically predicted

Table 2. Relative energies [kcal mol^{-1}] for stationary points in the reaction of methylthiyl radical (**10**) with complexes **27**, **32**, **37**, and **42**.

Structure	ΔE [UHF/DZP]	ΔE [B3LYP/LB //UHF/DZP]	ΔE [B3LYP/DZP]	ΔE [B3LYP/LB //B3LYP/DZP]
10 + **27**	0.0	0.0	0.0	0.0
29	−8.6	−11.4	−19.9	−15.6
30	+5.7	−15.9	−8.6	−11.3
31	−3.6	−13.1	−10.9	−13.2
13 + **28**	+6.3	−4.0	+1.8	−3.7
10 + **32**	0.0	0.0	0.0	0.0
34	−7.0	−6.8	−8.7	−6.8
35	+23.2	−1.2	+3.2	−1.8
36	+8.2	−1.8	+1.6	−2.9
13 + **33**	+14.5	+4.6	+10.2	+3.7
10 + **37**	0.0	0.0	0.0	0.0
39	−7.3	−9.4	−13.9	−13.3
40	+37.4	+14.8	+19.4	+13.1
41	+11.4	+1.6	−6.3	−14.2
13 + **38**	+19.9	+11.5	+9.3	+1.6
10 + **42**	0.0	0.0	0.0	0.0
44	−3.8	−3.3	−5.6	−4.0
45	+31.9	+10.0	+15.9	+10.4
46	+11.1	+1.7	+3.8	−0.5
13 + **43**	+15.1	+4.8	+8.8	+3.1

difference in C–H bond energies between methanol and sodium methoxide cited above.[11] Reaction between radical **10** and complex **27** is initiated through formation of a strongly bound ternary complex **29**. Complexation of radical **10** involves formation of a weak hydrogen bond between the negatively charged oxygen atom and the methyl group of radical **10**. Considering this structure, the complexation energy of over 15 kcal mol^{-1} is surprisingly large. Inspection of the charge and spin-density distribution reveals, however, that the complexation energy is not due to hydrogen-bond formation, but to transfer of approximately one third of the negative charge to the sulfur atom. This is accompanied by transfer of unpaired spin density in the opposite direction. Complex **29** might therefore best be described as a resonating thiol radical + alkoxy anion/thiolate + alkoxy radical pair. This result should be viewed with some caution as density functional methods have predicted delocalized wavefunctions in symmetric open-shell systems to be artificially stable before.[17] The transition state for hydrogen abstraction **30** is located 4.3 kcal mol^{-1} above reactant complex **29**. The structure of **30** (Figure 2) is distinctly different from that of the corresponding neutral transition state **20**. Comparison of the S–H bond length in **30** of 1.36 Å with the same bond length in methyl thiol (**10**) of 1.35 Å shows that the hydrogen-transfer process is fully complete. The small imaginary frequency of only −136 cm^{-1} describes a sliding movement of the S–H bond from the newly generated radical center to the negatively charged oxygen atom. The product complex **31** reached after descending from transition state **30** is 1.9 kcal mol^{-1} more favorable and includes the newly formed hydrogen bond between thiol and the negatively charged oxygen atom. According to the spin- and charge-density distribution, **31** is a ketyl radical anion stabilized through multiple hydrogen bonds. The unpaired spin density resides almost exclusively on the ketyl C–O group. The product

0947-6539/99/0510-3050 $ 17.50+.50/0 *Chem. Eur. J.* **1999**, *5*, No. 10

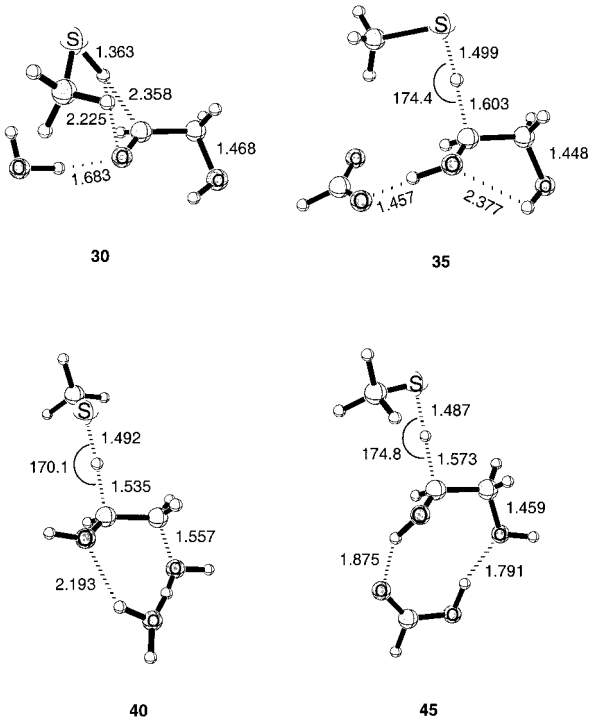

Figure 2. Transition states (**30**, **35**, **40**, and **45**) for the hydrogen abstraction from the anionic complexes **27** and **32**, the cationic **37**, and neutral complex **42**, respectively, by methyl thiyl radical **10** as optimized at the B3LYP/DZP level. Distances are given in Å.

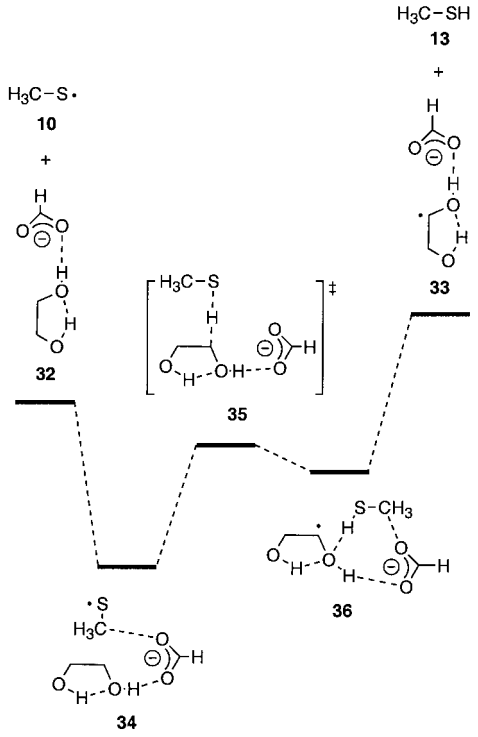

Scheme 6.

complex **31** is 2.4 kcal mol^{-1} less favorable than reactant complex **29**, which stands in remarkable contrast to the overall exothermic reaction.

We can conclude that a strongly basic catalyst capable of deprotonation of the substrate makes the overall C–H bond activation process reaction exothermic. The reaction from reactant to product complex remains, however, endothermic which appears to be due to formation of an (artificially?) resonance-stabilized reactant complex.

Formate as a catalyst: A more appropriate model for the base-catalyzed C–H bond activation in RNR, in terms of the strength of the base available for catalysis, is composed of the formate – ethylene-glycol complex **32** and methyl thiyl radical **10** (Scheme 6). In contrast to hydroxide studied before, formate is not basic enough to deprotonate ethylene glycol. Complex **32** is characterized through a strong, anionic hydrogen bond. In order to model the situation present in the RNR active site, at least to some extent, the conformation chosen in **32** features a formate anion hydrogen bonded to one hydroxy group, while the second hydroxy group forms an intramolecular hydrogen bond in the ethylene-glycol moiety. The complexation energy for formation of **32** from formate and ethylene glycol is $E_{compl} = -23.5$ kcal mol^{-1}; this value is significantly more than for the complex between formate and water ($E_{compl} = -17.0$ kcal mol^{-1}) calculated at a similar level of theory.[18] The difference between these two values is likely to stem from the fact that the intramolecular hydrogen bond between the two glycol hydroxy groups becomes significantly shorter and thus stronger upon complex formation. Efforts to locate stationary points, in which proton transfer has occurred from ethylene glycol to formate have not been successful. Upon optimization all these structures revert back to **32**, indicating a single-minimum potential energy surface for proton transfer between formate and ethylene glycol in **32**. Hydrogen-atom abstraction from the carbon atom closest to the hydrogen-bonded hydroxyl group through radical **10** yields radical anion **33** and methyl thiol (**13**). Comparison of the complexation energies for formation of **32** and **33** indicates that **33** is bound more strongly by $\Delta E_{compl} = 3.4$ kcal mol^{-1}. This is also born out by the length of the intermolecular hydrogen bond, which is reduced significantly on going from **32** (1.641 Å) to **33** (1.519 Å). The more favorable complexation energy for formation of **33** translates directly into a less endothermic C – H bond activation process relative to the uncatalyzed process. The overall reaction is, however, still endothermic by +3.7 kcal mol^{-1}. The C–H bond activation process is initiated through formation of ternary complex **34**. As in anionic complex **29** (Scheme 5) the methyl thiyl radical coordinates through its methyl hydrogen atoms to the center of negative charge located on the formate oxygen atoms. In contrast to **29**, however, the unpaired spin density is localized exclusively on the sulfur atom in **34** and the CH_3S moiety carries practically no excess negative charge. This arrangement is actually quite similar to that found in the X-ray structure of guanosine diphosphate bound in the active site of the *E. coli* R1 protein.[19] The reaction then proceeds through transition state **35** located 5.1 kcal mol^{-1} above complex **34**, before reaching product complex **36**. The energy difference between the reactant complex **34** and the product complex **36** amounts to +3.9 kcal mol^{-1}, which is rather close to the overall reaction energy of +3.7 kcal mol^{-1}. How effective is base catalysis through formate? The intracomplex

reaction barrier for the *uncatalyzed* C–H bond activation of ethylene glycol is $+12.7$ kcal mol^{-1}, which is reduced to $+5.1$ kcal mol^{-1} in the presence of formate. This barrier lowering of 7.6 kcal mol^{-1} is significantly larger than the base-induced reduction of the reaction endothermicity, and we can safely conclude that formate acts as a true catalyst. Inspection of structural characteristics of **35** (Figure 2) shows that not only the reduced reaction endothermicity but also the decreased barrier height are based on variations in the hydrogen bond strength. The length of the formate–glycol hydrogen bond is only 1.457 Å in transition state **35**, significantly shorter than in both the reactant or the product complexes. Taking the length of a hydrogen bond in a series of related systems as an indicator of its strength, this would imply that the hydrogen bond is strongest in **35**, followed by **36** and **34**. One consequence of increased hydrogen bonding appears to be an enhancement of the charge-transfer interaction between substrate and the thiyl radical in **35**. The cumulative charge of the CH_3S moiety in **35** is -0.24 e, which is substantially more negative than in the neutral transition state **20**. The strength of hydrogen bonding can also be estimated as the energy difference between the complexes **32**, **33**, **35**, and the corresponding neutral systems plus formate. This approach must be viewed with some caution when applied to transition states, as the structure of transition states is likely to change significantly more upon complexation than that of ground states. Using this approach, we obtain complexation energies of -23.5, -35.2, and -25.9 kcal mol^{-1} for structures **32**, **35**, and **33**, respectively. Compared with the ground states **32** and **33**, the hydrogen bond strength for transition state **35** appears overly large at more than 35 kcal mol^{-1}. This value might also include the ion–dipole interaction energy between formate and the methyl thiol radical. If we assume a value of -4.3 kcal mol^{-1} for this component,[20] we would still arrive at a hydrogen bond strength of -30.9 kcal mol^{-1} in transition state **35**, over 7 kcal mol^{-1} more than in the ground state complex **32**. As discussed already for **32**, the intramolecular hydrogen bond formed between the two glycol hydroxy groups might also contribute to the formal value of the hydrogen bond strength in **35**. All this illustrates is that hydrogen bond energies in excess of 27 kcal mol^{-1} are likely to be the result of multiple interactions, which cannot easily be associated with a *single* hydrogen bond.[21] This result might also be important in other reactions, in which catalysis through short strong hydrogen bonds has been assumed to be substantial, if not essential.[22]

Several other complexes can be formed between ethylene glycol and formate. The most stable complex appears to be **32b**, in which both ethylene-glycol hydroxy groups form hydrogen bonds to formate. This arrangement is 2.9 kcal mol^{-1} more stable than complex **32**. Even though **32b** might not be too good a model for the situation in the RNR-binding pocket, we have also studied the C–H bond activation process starting from **32b**. The corresponding transition state **35b** is more stable than **35** by 0.9 kcal mol^{-1}, while the product complex **33b** is actually less favorable than **33** by 0.1 kcal mol^{-1}. Comparison of the energy differences between **32b** and **35b** (bifurcated arrangement) and between **32** and **35** (end-on arrangement) shows that the reaction barrier is lower for the end-on arrangement by 2.0 kcal mol^{-1}. This implies that binding of the substrate in a bifurcated fashion will lead to a much less efficient C–H functionalization step.

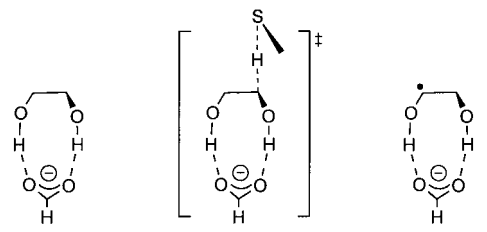

32b **35b** **33b**

In conclusion we have found here that complete deprotonation of the substrate in the RNR-catalyzed C–H bond activation process is not necessary in order to achieve a substantial reduction of the reaction barrier. The remarkable catalytic effect exerted by formate appears to be due to a modulation of the strength of the anionic hydrogen bond along the reaction pathway such that the transition state is stabilized most efficiently.

Hydronium cation as a catalyst: As discussed in the introduction already, general acid catalysis represents the second alternative for acceleration of water elimination from radical **2** generated in the RNR active site. In order to study the influence of acidic residues present in the RNR active site on the C–H bond activation step, the reaction between methyl thiyl radical and ethylene glycol has been reinvestigated in the presence of H_3O^+. The most stable complex formed between H_3O^+ and ethylene glycol has a bridged structure (**37**; Scheme 7). Structures in which H_3O^+ is bound to only one of the glycol hydroxy groups are not only less favorable energetically, but will also be inferior models for the RNR-catalyzed process of interest here.

Reaction between radical **10** and complex **37** leads to methyl thiol (**13**) and complex **38** as the products. As has been predicted before in a theoretical study of the solution behavior of alkene radical cations,[8] the direct hydrogen-abstraction product obtained from **37** does not represent a stable species and relaxes immediately to a structure that can best be viewed as the ion–dipole complex between the acetaldehyde-enol radical cation and the water dimer. Thus, the process of C–H bond activation in the presence of a suitably strong general acid is intimately coupled to protonation and dissociation of the β-hydroxy substituent. This has a marked effect on the overall reaction thermochemistry, which at $\Delta E_{rxn} = +1.6$ kcal mol^{-1} is 5.5 kcal mol^{-1} more favorable than for the neutral reference system. The ion–dipole complex formed between radical **10** and reactant complex **37** is characterized by an ionic hydrogen bond between the sulfur atom and ethylene glycol. Formation of complex **39** is accompanied by an intramolecular proton-transfer reaction such that one of the ethylene-glycol oxygen atoms becomes the formal center of positive charge. In stark contrast to the anionic systems investigated before, however, formation of a strongly bound substrate complex and the much more favorable reaction energy do not translate into transition-state stabilization here. Transition state **40** for C–H bond

0947-6539/99/0510-3052 $ 17.50+.50/0 *Chem. Eur. J.* **1999**, *5*, No. 10

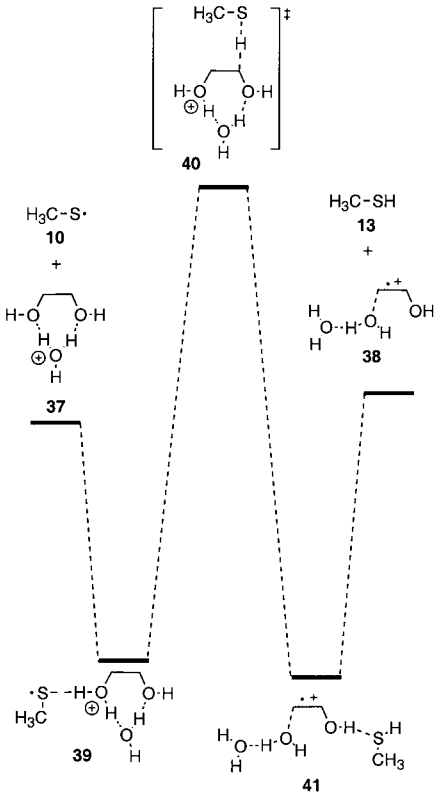

Scheme 7.

activation is located 26.4 kcal mol^{-1} above reactant complex **39** and 13.1 kcal mol^{-1} above the separated reactants **10** and **37**. The large energy difference between **39** and **40** is, at least in part, due to the hydrogen bond between the sulfur radical center and cationic glycol substrate that is present in **39** but absent in **40**. This effect alone cannot explain, however, why the reaction barrier relative to the separate reactants is actually *larger* in the cationic system by almost 3 kcal mol^{-1} as compared with the neutral system. This is the more surprising as lengthening of the β-C–O bond in **40** is clearly visible. This implies that the C–H bond activation step through **40** is tightly coupled to the exothermic elimination of the β-hydroxy group. The main cause of the high reaction barrier appears to be the electrophilic nature of the methyl thiyl radical, which carries a positive charge of $+0.04$ e in **40**, a small negative charge in all neutral transition states, and a substantial negative charge in all anionic systems studied here.

Formic acid as a catalyst: Siegbahn[9] has recently suggested that C–H bond activation is also accelerated through neutral acids such as formic acid. In order to compare this option to the other systems studied here, we have also studied the C–H bond activation in ethylene glycol in the presence of formic acid as catalyst (Scheme 8). The most stable complex formed between catalyst and substrate is **42**, in which formic acid bridges across the two glycol hydroxy groups through the formation of two hydrogen bonds. Hydrogen-atom transfer from the methylene group adjacent to the hydroxy group that donates a hydrogen bond to formic acid yields the most stable product complex **43**. This reaction is slightly endothermic at $+3.1$ kcal mol^{-1}, 3.5 kcal mol^{-1} more favorable than the uncatalyzed reaction. Hydrogen abstraction is, of course, also possible from the other methylene group in **42**. However, the product complex formed in such a step is 8.0 kcal mol^{-1} less favorable than **43**, and this process was therefore not investigated in more detail. The most stable complex formed between radical **10** and **42** is **44**, in which a hydrogen bond has been formed between the sulfur center and one of the glycol hydroxy groups. The reaction then proceeds through transition state **45**, located 14.4 kcal mol^{-1} above the reactant complex, to product complex **46**. The structure of **45** (Figure 2) is very similar to that of **20**, the transition state of the uncatalyzed process, and does not show the β-C–O bond lengthening observed in cationic transition state **40**.

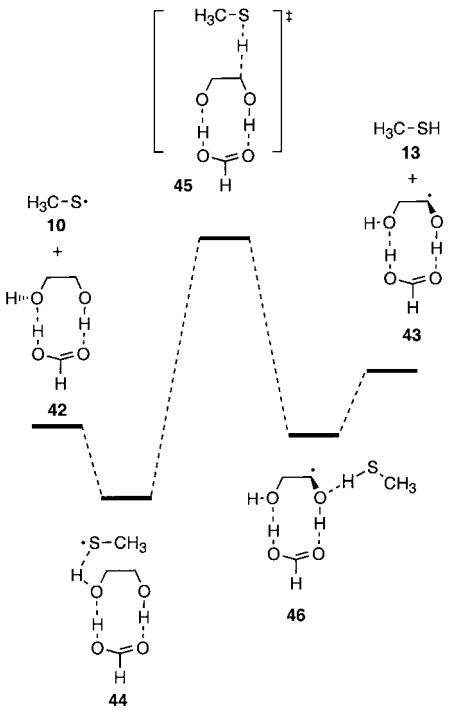

Scheme 8.

Discussion and Conclusion

How do the results obtained in this computational study relate to the RNR-catalyzed C–H bond activation? The very first step in the RNR-catalyzed process consists of binding the negatively charged di- or triphosphate substrate into the binding pocket. We can hardly expect that our minimal model systems will predict the energetic or structural characteristics of this process even in a qualitative manner. The main contribution that we can hope to obtain from small model studies of the RNR mechanism is that of the actual hydrogen-atom-transfer step in the preformed reactant complexes. We have therefore collected in Table 3 the intracomplex reaction barriers $\Delta E_C^{\neq}$, that is, the energy difference between reactant complex and transition state, for all model systems studied here. It can easily be seen that activation of substrate **22** is more facile relative to **17** or **11**. The most effective catalyst appears to be OH^- as it lowers the reaction barrier for activation of ethylene glycol from 12.7 to 4.3 kcal mol^{-1}. A

Table 3. Intracomplex activation barriers $\Delta E_C^{\neq}$, reaction energies $\Delta E_{RXN,C}$, and intrinsic barriers $\Delta E_{0,C}^{\neq}$ [kcal mol^{-1}]

Substrates	$\Delta E_C^{\neq}$	$\Delta E_{RXN,C}$	$\Delta E_{0,C}^{\neq}$
11	+13.4	+8.4	+8.7
17	+12.7	+6.9	+8.9
22	+11.7	+6.8	+7.3
17 + OH^-	+4.3	+2.4	+3.0
17 + HCO_2^-	+5.0	+3.9	+2.7
17 + H_3O^+	+26.4	−0.9	+26.9
17 + HCO_2H	+14.4	+3.5	+12.6

substantial part of this barrier lowering is, of course, due to changes in reaction thermochemistry as can readily be seen from the intracomplex reaction energies $\Delta E_{RXN,C}$, that is, the energy difference between the product and reactant complex. In order to separate the influence of the catalytically active species on the reaction barrier from that on the reaction thermochemistry, we have analyzed the data contained in Table 3 with the aid of a Marcus-type equation [Eq. (1)], which is obtained from the original Marcus equation through substitution of free energies ΔG by potential energy differences ΔE.

$$\Delta E_C^{\neq} = \Delta E_{0,C}^{\neq} + 0.5\,\Delta E_{RXN,C} + \frac{(\Delta E_{RXN,C})^2}{16\,\Delta E_{0,C}^{\neq}} \quad (1)$$

Equation (1) describes a reaction series with constant intrinsic barrier $\Delta E_{0,C}^{\neq}$, which is modified by two terms responsible for the variable thermochemistry of the reaction to yield the true reaction barrier $\Delta E_C^{\neq}$. Using Equation (1), we can extract the intrinsic barrier for a hypothetical thermoneutral process and isolate the influence of the catalyst on the actual barrier formation from the data in the first two columns in Table 3. The intrinsic barriers $\Delta E_{0,C}^{\neq}$ derived in this way are given in the third column in Table 3. Comparison of the intrinsic barriers for the two base-catalyzed processes shows that formate is the more efficient catalyst as it yields the largest reduction in intrinsic barrier relative to the uncatalyzed case. The cationic system, in contrast, has a huge intrinsic barrier, and even for neutral formic acid the reaction barrier is significantly higher than for the uncatalyzed case. In conclusion the theoretical model studies presented here suggest that there might be several reasons for class I and II RNRs to evolve a base-catalyzed mechanism of ribonucleotide reduction. Besides the facile elimination of water from 1,2-hydroxyalkyl radicals in a general base-catalyzed fashion,[2] we have found here that the preceding radical-forming step also benefits greatly from the presence of a basic residue. This effect appears to be due to formation of a strong hydrogen bond between the C3′-hydroxy group and the catalytically active base. The strength of this hydrogen bond is modulated such that the strongest and, therefore, the shortest hydrogen bond is formed in the transition state.

Acknowledgments

This work was supported by the Zentraleinrichtung Rechenzentrum der TU Berlin, the Konrad-Zuse-Zentrum für Informationstechnik Berlin, and the Leibniz-Rechenzentrum München through generous allocations of computer time, and by the Fonds der Chemischen Industrie.

[1] a) J. Stubbe, *Adv. Enzymol. Relat. Areas Mol. Biol.* **1990**, *63*, 349; b) J. Stubbe, *J. Biol. Chem.* **1990**, *265*, 5329; c) J. Stubbe, W. A. van der Donk, *Chem. Biol.* **1995**, *2*, 793; d) J. Stubbe, W. A. van der Donk, *Chem. Rev.* **1998**, **98**, 705.
[2] R. Lenz, B. Giese, *J. Am. Chem. Soc.* **1997**,*119*, 2784.
[3] B.-M. Sjöberg, *Struct. Bonding* **1997**, *88*, 139.
[4] M. Lammers, H. Follmann, *Struct. Bonding* **1983**, *54*, 27.
[5] P. Nordlund, H. Eklund, *J. Mol. Biol.* **1993**, *232*, 123.
[6] a) B. C. Gilbert, J. P. Larkin, R. O. C. Norman, *J. Chem. Soc. Perkin 2* **1972**, 794; b) A. J. Dobbs, B. C. Gilbert, R. O. C. Norman, *J. Chem. Soc. Perkin 2* **1972**, 786; c) K. M. Bansal, M. Grätzel, A. Henglein, E. Janata, *J. Phys. Chem.* **1973**, *77*, 16; d) S. Steenken, M. J. Davies, B. C. Gilbert, *J. Chem. Soc. Perkin 2* **1986**, 1003.
[7] S. Steenken, *J. Phys. Chem.* **1979**, *83*, 595.
[8] H. Zipse, *J. Am. Chem. Soc.* **1995**, *117*, 11798.
[9] P. Siegbahn, *J. Am. Chem. Soc.* **1998**, *120*, 8417.
[10] D. Griller, J. M. Kanabus-Kaminska, A. Maccoll, *J. Mol. Struct.* **1988**, *163*, 125.
[11] M. L. Steigerwald, W. A. Goddard III, D. A. Evans, *J. Am. Chem. Soc.* **1979**, *101*, 1994.
[12] N. Godbout, D. R. Salahub, J. Andzelm, E. Wimmer, *Can. J. Chem.* **1992**, *70*, 560.
[13] a) A. D.Becke, *J. Chem. Phys.* **1993**, *98*, 5648; b) C. Lee, W. Yang, R. G. Parr, *Phys. Rev. B* **1988**, *37*, 785; c) R. H. Hertwig, W. Koch, *J. Comp. Chem.* **1995**, *16*, 576.
[14] M. J. Frisch, G. W. Trucks, H. B. Schlegel, P. M. W. Gill, B. G. Johnson, M. A. Robb, J. R. Cheeseman, T. Keith, G. A. Petersson, J. A. Montgomery, K. Raghavachari, M. A. Al-Laham, V. G. Zakrzewski, J. V. Ortiz, J. B. Foresman, J. Cioslowski, B. B. Stefanov, A. Nanayakkara, M. Challacombe, C. Y. Peng, P. Y. Ayala, W. Chen, M. W. Wong, J. L. Andres, E. S. Replogle, R. Gomperts, R. L. Martin, D. J. Fox, J. S. Binkley, D. J. Defrees, J. Baker, J. P. Stewart, M. Head-Gordon, C. Gonzalez, J. A. Pople, *Gaussian 94, Revision E.1*, Gaussian, Pittsburgh PA, **1995**.
[15] MOLPRO 96 is a package of ab initio programs written by H.-J. Werner and P. J. Knowles, with contributions from R. D. Amos, A. Berning, D. L. Cooper, M. J. O. Deegan, A. J. Dobbyn, F. Eckert, C. Hampel, T. Leininger, R. Lindh, A. W. Lloyd, W. Meyer, M. E. Mura, A. Nicklass, P. Palmieri, K. Peterson, R. Pitzer, P. Pulay, G. Rauhut, M. Schütz, H. Stoll, A. J. Stone, and T. Thorsteinsson.
[16] J. W. Ochterski, G. A. Petersson, K. B. Wiberg, *J. Am. Chem. Soc.* **1995**, *117*, 11299.
[17] a) T. Bally, G. N. Sastry, *J. Phys. Chem. A*, **1997**, *101*, 79223; b) Y. Zhang, W. Yang, *J. Chem. Phys.* **1998**, *109*, 2604; c) M. Sodupe, J. Bertran, L. Rodriguez-Santiago, E. J. Baerends, *J. Chem. Phys. A* **1999**, *103*, 166.
[18] Y. Pan, M. A. McAllister, *J. Am. Chem. Soc.* **1997**, *119*, 7561.
[19] M. Eriksson, U. Uhlin, S. Ramaswamy, M. Ekberg, K. Regnström, B.-M. Sjöberg, H. Eklund, *Structure* **1997**, *5*, 1077.
[20] This value is obtained from the difference in reaction energies for formation of complexes **34** (−6.8 kcal mol^{-1}) and **19** (−2.5 kcal mol^{-1}) from free methyl thiol radical and the substrate.
[21] A value of $E_{compl} = -27.2$ kcal mol^{-1} has been calculated for formation of the formate–formic acid complex.[18]
[22] a) A. J. Kirby, *Acc. Chem. Res.* **1997**, *30*, 290; b) A. Warshel, A. Papazyan, *Proc. Natl. Acad. Sci. USA* **1996**, *93*, 13665; c) S. Shan, D. Herschlag, *Proc. Natl. Acad. Sci. USA* **1996**, *93*, 14474; d) S. Shan, D. Herschlag, *J. Am. Chem. Soc.* **1996**, *118*, 5515; e) P. A. Frey, S. A. Whitt, J. B. Tobin, *Science* **1994**, *264*, 1927; f) W. W. Cleland, M. M. Kreevoy, *Science* **1994**, *264*, 1887.

Received: February 9, 1999 [F1599]

